INFLUENCE OF ELECTRON SOURCES ON THE NEAR-FIELD PLUME IN A MULTISTAGE PLASMA THRUSTER

Duras J.[a,b,*], Schneider R.[a], Kalentev O.[d], Kemnitz S.[c,e], Matyash K.[c], Koch N.[b], Lüskow K.[a], Kahnfeld D.[a], Bandelow G.[a]

[a] *Institute of Physics, Ernst-Moritz-Arndt University of Greifswald, D-17498 Greifswald, Germany*

[b] *Department of Applied Mathematics, Physics and Humanities, Nürnberger Institute of Technology, D-90489 Nürnberg, Germany*

[c] *Computing Center, Ernst-Moritz-Arndt University of Greifswald, D-17498 Greifswald, Germany*

[d] *Biomedizinische NMR Forschungs GmbH am Max-Planck-Institut für biophysikalische Chemie, D-37077 Göttingen, Germany*

[e] *University Rostock, Institute of Informatics, D-18059 Rostock, Germany*

[*] `julia.duras@uni-greifswald.de`

Abstract. In order to obtain a better understanding of the near-field plume of a multistage plasma thruster, the influence of an external electron source is investigated by Particle-In-Cell simulations. The variation of the source position showed a strong influence of the magnetic field configuration on the electron distribution and therefore on the plume plasma. In the second part of this work, higher energetic electrons were injected in order to model collision-induced diffusion in the plume. This broadens the electron distribution, which leads to a more pronounced divergence angle in the angular ion distribution.

Keywords: Multistage plasma thruster, near-field plume, external electron source, Particle-In-Cell.

1. Motivation

Ion thrusters with magnetic plasma confinement can be optimized by modifying magnetic field configuration, anode potential, neutral gas source and neutralizer properties. In the case of neutralizer adjustment, mainly the plume behavior is influenced. For a better understanding of the near-field plume physics, the influence of an external electron source on its properties is studied. Here, position and source distribution are varied and the interaction between magnetic field, potential and plasma densities are investigated.

For this purpose a multistage plasma thruster similar to the HEMP thruster [1], [2] was simulated with the Particle-In-Cell method.

2. Physics of a multistage plasma thruster

A multistage plasma thruster consists of a rotationally symmetric discharge channel with an anode and an inlet for the propellant at the upstream end, as shown in figure 1. The discharge channel is surrounded by axially magnetized permanent magnet rings with opposite magnetization. Inside the thruter channel a dielectric wall is facing the plasma. At the exit a grounded pole piece is placed. Outside the thruster channel a hollow cathode neutralizer is placed. It provides the thruster with starter electrons for igniting the discharge and neutralizes the out-going ion beam. The permanent magnets generate a magnetic field which points mainly in axial direction especially
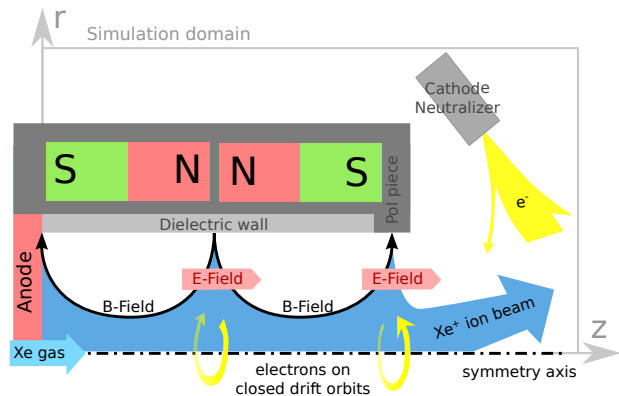

Figure 1. Scheme of HEMP-like thrusters, similar to [3].

in the channel region next to the symmetry axis. In the so-called cusp regions, the magnetic field next to the channel wall is mostly directed in radial direction. In figure 1 three cusps are shown, an anode cusp, an inner cusp and an exit cusp. The magnetic field strength B is chosen such that the Larmor radius of the electrons is much smaller than the radius of the discharge channel, while for the ions it is larger $r_{\mathrm{L,e}} \ll R < r_{\mathrm{L,i}}$. Therefore, in the thruster channel electrons are magnetized while ions are not. Electrons are created by the neutralizer acting as cathode and experience close to the axis a magnetic field nearly parallel to the axis which directs them towards the anode.

The cusp-structure of the magnetic field builds up

a magnetic mirror in front of the thruster exit. In combination with the potential drop, this magnetic mirror lets the electrons oscillate in a confined electron cloud in the plume originating from the electron source pointing towards the thruster's exit. In the cusp regions, the perpendicular electric and magnetic fields induce a $\vec{E} \times \vec{B}$-drift to the electrons in poloidal direction. In addition the magnetic field configuration builds up a magnetic mirror in radial direction and the electrons are reflected before they reach the channel wall. The strong radial magnetic field in these regions separate the different thruster regions. Only few electrons can overcome these regions by collisional and anomalous transport, which is caused by electrostatic turbulence [4]. By this, electron density is increased in the respective downstream cusp region and allows for efficient ionization of the propellant. In the channel regions between the cusps, the electron transport is determined in axial direction by the fields and in radial direction by collisional transport. Therefore, in the regions where no cusps are existing electron losses at the dielectric wall are low and the non-magnetized ions can generate a positive surface charge. The dominance of the axial transport along the magnetic field lines quickly compensates small perturbations of the electric potential and results in a flat potential inside the discharge channel with only small steps at the regions with large radial transport, namely at the cusps. Xenon ions follow the potential gradients and are getting accelerated mostly in the potential drop of the thruster exit. Within the acceleration channel the radial potential gradients towards the wall are rather small and the ion energies are kept below the sputter threshold, hence minimizing erosion. The different dynamics for electrons and ions lead to a spatial separation of ionization in the channel and acceleration at the thruster exit. In order to produce an ion beam with small divergence angle, a grounded magnetic pole piece is placed at the exit cusp. The magnetic field lines are focused in this region and the grounded potential produces in radial direction a large potential drop of $\Delta\phi = eU_a$. This guides the electrons to enter the thruster channel and get confined only close to the symmetry axis, which creates an ion lens. The resulting ion beam is strongly affected by the potential structure in this region as well as in the near-field plume region. Here, the magnetized electrons are determining the potential and therefore influencing the ion trajectories.

Therefore, the thruster magnetic field topology and the potential in the plume are important for optimization of the ion beam divergence. Different external electron source positions might change the electron distribution in the plume and therefore potential and angular ion distribution.

3. Code description and simulation set-up

The non-Maxwellian characteristics of the electron distribution function in the thruster requires a kinetic method [5]. Due to the rotational symmetry of the system, the spatial domain was reduced to r-z and an electrostatic 2d3v Particle-In-Cell code with Monte Carlo collisions (PIC MCC) [6], [4] was used. In this PIC-MCC simulation we follow the kinetics of so-called Super Particles (each of them representing many real particles), moving in the self-consistent electric field calculated on a spatial grid by solving Poisson's equation. The particle collisions are treated by Monte Carlo Collision (MCC) routines. All relevant collisions are included in the model: electron-electron Coulomb, electron-neutral elastic, ionization and excitation collisions, ion-neutral momentum transfer and charge exchange collisions. The dynamics of the background neutral gas is self-consistently resolved by Direct Simulation Monte Carlo [7]. Plasma surface interactions are provided by a Monte Carlo erosion module. For electrons an anomalous transport model is applied [8]. In order to reduce the computational time a similarity scaling is applied with a factor of 10 [9].

In figure 1, the simulation domain and the thruster geometry are shown. The thruster has a channel radius of $R = 9\,\mathrm{mm}$ and length of $L = 51\,\mathrm{mm}$. The main part of the channel wall is dielectric, at the exit a grounded magnetic pole piece terminates the thruster channel. At the anode a potential of $U_a = 500\,\mathrm{V}$ is applied. The simulated domain consists of a fine grid of 890×240 cells with a grid spacing of $\Delta r = \Delta z = 0.5\lambda_{D,e} = 0.01\,\mathrm{mm}$ containing the thruster channel and the near field plume. It is overlaid by a courser grid of four times larger cell size, covering the whole domain. The potential boundary condition at the symmetry axis and at the right hand side of the domain is set to zero radial electric field, while at other domain boundaries Dirichlet boundary conditions with $\phi = 0\,\mathrm{V}$ or $\phi = U_a$ are applied. For the grounded magnetic pole piece the potential is set to zero. The solution at the domain boundary between fine and coarse mesh is transferred explicitly by boundary conditions between the two meshes.

4. Results

4.1. Influence of the electron source position

Within PIC ion thruster simulations, the resolved domain is usually too small to simulate the neutralizer at the position of the experiment. Due to the magnetization of the electrons the usage of an effective source, placed at the same magnetic field line as the neutralizer is used. The external source is simulated as a volume source of size $4\,\mathrm{mm} \times 4\,\mathrm{mm}$ with Maxwellian distributed electrons of a temperature of $T_e = 2\,\mathrm{eV}$ and a cathode current of $I_{\mathrm{cath}} = 1.5\,\mathrm{mA}$.

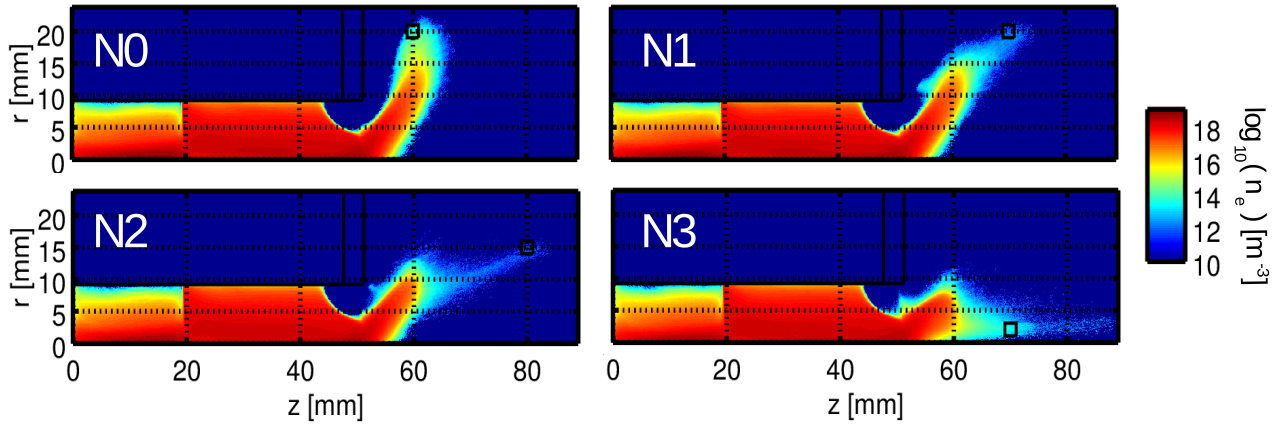Four different source positions were chosen in order

Figure 2. Electron density in logarithmic scale for different source positions.

to study its influence on the plume plasma. In figure 2 the resulting electron density is shown and the black box in the plume indicates the electron source position. The magnetic field lines where the sources N0 and N1 are located, are connected to the front of the metal cap. Sources N2 and N3 aim at the thruster exit. The positions where also chosen to represent different magnetization strengths of the source electrons. While the B-field strengths at positions N1 and N3 are similar, it is nearly doubled at N0 and nearly the half at N2.

In figure 2 the electron density for the different source position is shown in logarithmic scale. The simulated time to reach steady state was in the range of 2–6 µs, which corresponds to a computation time of 20 up to 60 days. For the four cases the channel plasma is practically not changing. At 20 mm the central cusp is clearly visible, as well as the dominant axial transport by the magnetic field lines close to the z-axis, which produces a higher density. Due to the electron loss at the anode, the region between anode and central cusp is less filled than the region between the central and exit cusp, where both cusps act as sources of energetic electrons.

For the sources N0–N2, the electron distribution in the near-field plume and close to the exit is changing only in the low density range. The electron density in the range of $10^{18}\,\mathrm{m}^{-3}$, shown in red, is nearly constant. This distribution is built up by trapped electrons, oscillating between the magnetic mirror and the potential drop. For N2, with lowest magnetic field strength at its source position, electrons are getting accelerated by the potential, which results in a lower density. It increases in the region of higher B due to oscillation in the magnetic trap. In the case of N0, with highest magnetic field strength at the source position, this appears already in the source region and increases with increasing B. The electron distribution formed by source N1 shows a mixture of these two cases. Electrons injected by source N3 fill in a wider area due to the magnetic field configuration in this region.

Since the differences of the electron distribution generated by sources N0, N1 and N2 are only visible in the low density range, the resulting potentials are quite similar. Only the source position of N3 close to the axis shows an electron distribution expanded towards the symmetry axis. Therefore, the resulting potential, in the first row in figure 3, is given for N0 and N3. It clearly shows a flat potential in the channel, which drops in the plume. At the thruster exit the metal wall is forming a potential drop in radial direction which acts as a lens for the non-magnetized ions. For N3, in comparison to N0, the potential distribution in the plume is compressed in radial direction and stretched in axial direction. This is a result of the broader electron distribution close to the symmetry axis.

Since the ions are not magnetized they follow the potential gradient which determines their angular distribution. At the bottom row in figure 3 the corresponding ion densities for electron source N0 and N3 are shown in logarithmic scale. Within the channel the distribution satisfies very well quasi-neutrality, as expected for a plasma. At the thruster exit the potential drop accelerates the ions into the plume. Due to the different electron distributions in the plume, for N0 the distribution of higher ion density is expanding deeper into the plume than for N3. For the angular ion distribution, the influence of the different electron sources is minor, since in both cases ions show a broad distribution. Only close to the symmetry axis the contribution is higher for N3.

The magnetic field configuration in front of the thruster exit determines the distribution of electrons in the plume, whereas the source position influences the ion distribution in the plume only slightly.

4.2. Thermal versus beam-like electron source

Due to the long run time of PIC simulations, it is not possible to represent the full electron dynamics. In the plume electron and neutral density are two orders lower than in the channel with a typical Coulomb collision time of about 50 µs. Typically, for a runtime of
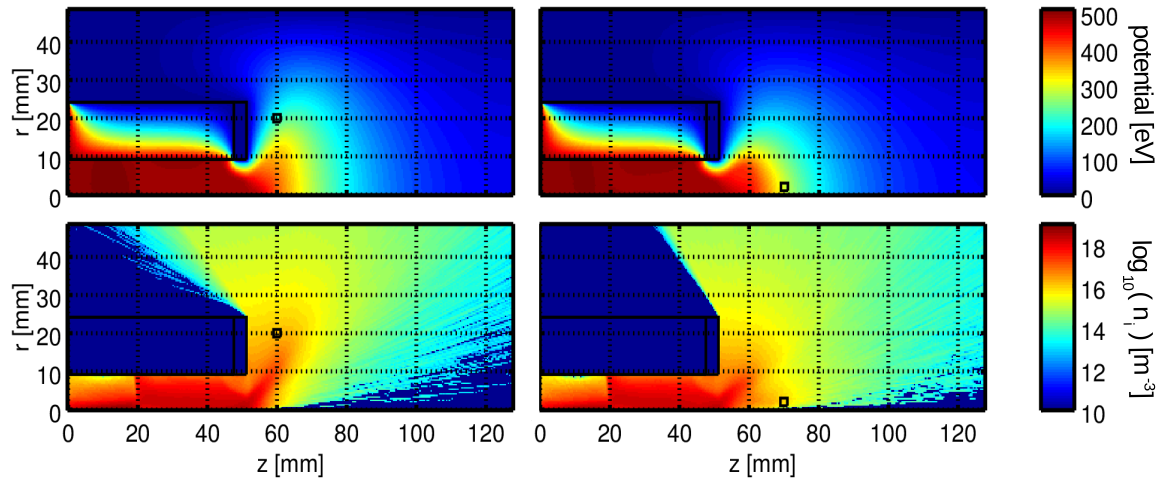
Figure 3. Potential and ion density generated by electron source N0 and N3. The ion density is given in logarithmic scale.

1 month a simulated time in the range of some micro seconds is possible, which does not resolve collision-induced electron diffusion. Therefore, the filling of the plume with electrons guaranteeing quasi-neutrality is not appearing as observed experimentally, as this happens only on the time-scale of collisional transport.

In order to investigate this effect an electron beam directed away from the thruster is used as external source. Electrons with a higher velocity have a larger Larmor radius, which broadens their distribution in the plume. To further reduce the influence of the magnetic mirror the source is placed in a region of low magnetic field strength, similar to the one at the source position of N2. The injected electron beam has a thermal energy of 0.1 eV and a drift velocity of 20 eV. It is directed down-stream the thruster plume, with an angle of 55° with respect to the symmetry axis. As before the cathode current is set to $I_{\mathrm{cath}} = 1.5\,\mathrm{mA}$. The resulting electron density, potential and ion density are shown in figure 4. Densities are given in logarithmic scale. The black box in the plume indicates the electron source position.

As in the previously studied cases, the shape of the electron distribution in the plume remains very similar. But due to the higher probability to cross magnetic field lines, the distribution is broader. Since the magnetic field lines guide the plume electrons into the thruster this results in a higher density at the thruster exit, which increases the collisional rate, filling up the channel volume. As can be seen in the potential plot in figure 4, the increased electron density in the plume extends the potential drop. This affects the ions, which just follow the potential gradients, and a beam with a more pronounced shape and a dedicated peak at around 60° divergence angle is developing. Due to the higher electron density in the channel and close to the exit, the ionization rate increases which increases the ion density, as can be seen in the bottom plot in figure 4.

In figure 5 the angular current distribution with respect to the symmetry axis is given for the two thermal sources N0 and N3 as well as for the beam-like electron source. This distribution is calculated at the outer domain boundary and the angle vertex refers to the thruster exit $z = 51\,\mathrm{mm}$ at $r = 0\,\mathrm{mm}$. It is given in ion current density within 5° normalized to the total measured ion current density. Both thermal sources produce a flat angular distribution, where for source N3, the higher ion density close to the symmetry axis contributes more at low angles. The more extended electron distribution in the plume generated by the beam-like source directed away from the thruster produces a clear ion beam. This is a characteristics which is also seen in experiments [8].

5. Conclusion

In this work the influence of external electron sources on the plume in a multistage plasma thruster was studied. A strong impact of the magnetic field on the electron distribution in the near field plume was observed, especially due to the magnetic mirror effect. The electron distribution was insensitive to the source position in case of a thermal electron source. Only an effective source close to the symmetry axis increases the electron density close to the axis, which leads to higher contribution in the angular current distribution at small angles. In order to overcome calculation time limits and to represent electron diffusion in the plume by collisions, a source of higher energetic electrons directed away from the source was simulated. This produces a broader distribution in the plume, its shape determined by the magnetic field lines. The broader filling produces a more extended potential drop, which generates a pronounced ion beam.

In the experiment this effect might be further increased due to a higher neutral background pressure. Also, secondary electrons produced by impinging ions at the vacuum vessel walls can influence the electron
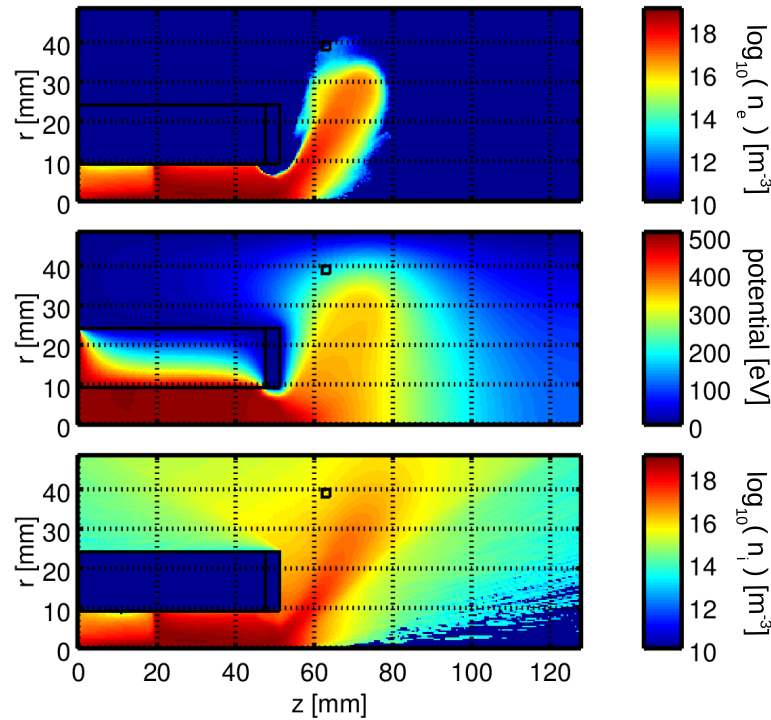
Figure 4. Electron density, potential and ion density for a beam-like electron source directed away from the thruster.
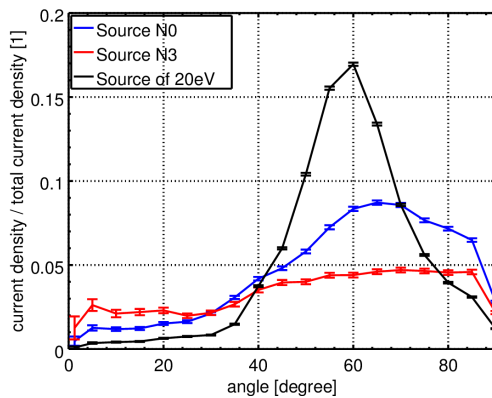

Figure 5. Angular current distribution with statistic error bars and angle given with respect to the symmetry axis.

distribution in the plume acting as additional near-axis source. Due to the magnetic field lines such electrons are guided towards the symmetry axis and would rise the angular current distribution at lower angles.

Acknowledgements

References

[1] G. Kornfeld, H. Seidel, and J. Wegener et al. Plasma Accelerator Arrangement, 1999. Priority: Germany No. 198 28 704.6, filed 26 June 1998.

[2] N. Koch, M. Schirra, and S. Weis et al. The HEMPT Concept - A Survey on Theoretical Considerations and Experimental Evidences . In *Proceedings of the 32nd International Electric Propulsion Conference*, number IEPC-2011-236, 2011.

[3] N. Koch, H.P. Harmann, and G. Kornfeld. Development and Testing Status of the THALES High Efficiency Multistage Plasma (HEMP) Thruster Family. In *Proceedings of the 29nd International Electric Propulsion Conference*, number IEPC-2005-297, 2005.

[4] O. Kalentev, K. Matyash, and J. Duras. Electrostatic Ion Thrusters - Towards Predictive Modeling . *Contributions to Plasma Physics*, 54:235–248, 2014.

[5] Karl Felix Lüskow. Physics of Ion Thrusters' Plumes . Master's thesis, University of Greifswald, July 2013.

[6] K. Matyash, R. Schneider, and A. Mutzke et al. Kinetic Simulations of SPT and HEMP Thrusters Including the Near-Field Plume Region. *IEEE Transactions on Plasma Since*, 38(9, Part 1):2274–2280, 2010.

[7] R. Procassini, C. Birdsall, E. Morese, and Cohen B. A relativistic monte carlo binary collision model for use in plasma particle simulation codes. *Memorandum No. UCB/ERL M87/24, University of California, Berkeley*, 1987.

[8] K. Matyash, O. Kalentev, and R. Schneider et al. Kinetic Simulation of the stationary HEMP thruster including the near-filed plume region. In *Proceedings of the 31st International Electric Propulsion Conference*, number IEPC-2009-110, September 2009.

[9] F. Taccogna, S. Longo, M. Capitelli, and R. Schneider. Self-similarity in Hall plasma discharges: Applications to particle models. *Phys. Plasmas*, 12:053502, 2005.